Material Realizations of Perfect Electric Conductor Objects

Ari Sihvola, Ismo V. Lindell, Henrik Wallén, and Pasi Ylä-Oijala

Department of Radio Science and Engineering
Aalto University School of Science and Technology
P.O. Box 13000, FI–00076 AALTO, Finland
ari.sihvola@tkk.fi, ismo.lindell@tkk.fi henrik.wallen@tkk.fi, pasi.yla-oijala@tkk.fi

Abstract – This article discusses the distinction between interfaces and boundaries in electromagnetics. Boundary conditions can be used to narrow down the computation domain of complex problems. However, terminating the space by a boundary condition is an approximation in real-world situations where fields penetrate across interfaces. To make this approximation accurate, the material parameters need to have a very strong contrast between the materials on the adjacent sides of the interface. In this article, the question is addressed how extreme the permittivity and permeability have to be in order to reasonably model a surface as a perfect electric conductor (PEC) boundary. It is argued that in addition to the large value of the permittivity, also a very small magnitude of the permeability is necessary in order to speed up the convergence of a material response towards the ideal PEC case.

Index Terms – Boundary conditions, extinction, extreme-parameter materials, metamaterials, PEC, scattering.

I. INTRODUCTION

In electromagnetics, the objective is often to solve electric and magnetic fields in a given region of space. Fields, due to a source, radiate and penetrate into the near and far surroundings, reacting to the environment, its structure, and boundaries. Sometimes, for reasons of decreasing the computational complexity and cost, the problems are formulated in a form that the domain of interest is bounded in which the fields need to be calculated. On the boundary of this domain, certain sufficient conditions for the fields have to be forced in order that the solutions are correct and non-ambiguous.

Boundary conditions simplify the solution process because one does not need to bother what happens on the other side of the boundary. On the other hand, when applied to model real-world situations, boundary conditions only approximate the electromagnetic effect of the material behind the surface. It is well known that replacing a dielectric boundary by an impedance condition is not exact or even accurate for an arbitrary field setting. This happens especially when the discontinuity of the material parameter contrasts over the interface is not very large.

It is essential to emphasize this fundamental difference between the interface problem and boundary problem (Figure 1). In the interface problem, the materials everywhere, on both sides of the interface, affect the fields in both domains. On the other hand, if the region 1 is terminated by a boundary condition, nothing behind this boundary can have any effect on the fields. In fact, it is senseless to talk about the region behind this boundary because it does not exist in the electromagnetic problem.

Despite this distinction, a connection exists between the two situations. Indeed, either of them can be approximated with the other one in certain cases. When such an approximation is taken, it is important to keep in mind which one of the pictures is primary. The first choice is that one treats the interface picture as a true model of the real world. Then it is possible to solve the electromagnetic problem in the interesting region by replacing the interface with a boundary and cutting away everything on the other side. This procedure can be termed as the *analytic* approach.

However, the complementary view is very important and useful: the boundary condition itself is primary. A great variety of different electromagnetic boundary conditions exist, and it is a legitimate

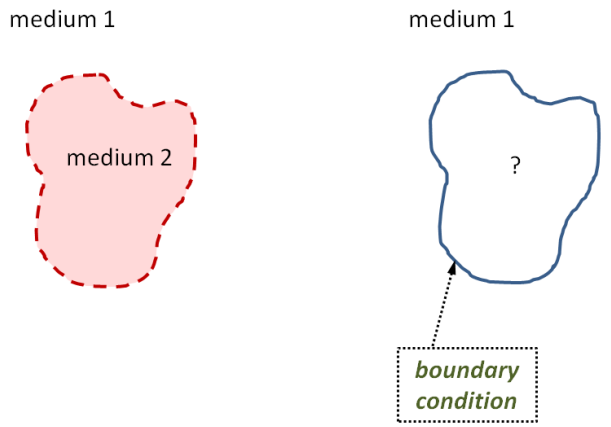

Fig. 1. The distinction between interface (left) and boundary (right) problems. In the latter case, there is nothing beyond the boundary.

project to study their properties in a systematic manner. Some of such ideal boundary conditions may turn out to display potential for interesting applications. For example, using such a concept, a desired antenna structure can be theoretically designed, and if the result is worth realizing, the next step is to synthesize it using composites or metamaterials. This procedure of starting from the boundary condition and proceeding to materials is called the *synthetic* approach.

Materials with extreme parameters are hence a natural choice for creating ideal boundaries. The term "extreme parameters" often refer to cases where one or more of the material parameters (permittivity, permeability, refractive index, and wave impedance) have either very small or very large values [1, 2]. Also anisotropic materials with certain components of the parameter tensors being extreme fall into this class. In the following, the effect of boundary conditions (in particular, the perfect electric boundary, PEC) is approximated by materials with isotropic extreme parameters, and the accuracy of the approximation is being estimated in quantitative terms.

II. EXAMPLES OF BOUNDARY CONDITIONS

Well-known boundary conditions are perfect electric conductor (PEC) and perfect magnetic boundary (PMC) conditions. In the former, the electric field component tangential to the surface vanishes ($\mathbf{n} \times \mathbf{E} = 0$), and the latter condition requires that the tangential magnetic field becomes zero ($\mathbf{n} \times \mathbf{H} = 0$). Here $\mathbf{n}$ is the unit normal pointing away from the boundary.

A generalization of PEC and PEC conditions is the impedance boundary condition [3] which defines the ratio between the tangential electric and magnetic fields on the surface. Another generalization is the so-called PEMC condition [4, 5] with one parameter M which states that the fields satisfy $\mathbf{n} \times (\mathbf{H} + M\mathbf{E}) = 0$. Furthermore, the so-called soft-and-hard surface [6] is characterized by another interesting pair of boundary conditions $\mathbf{v} \cdot \mathbf{E} = 0,\ \mathbf{v} \cdot \mathbf{H} = 0$, for a vector $\mathbf{v}$ along the boundary.

Also, field components normal to the boundary have been of interest in terms of surfaces [7]. The so-called DB boundary condition [8] requires that the normal components of the electric and magnetic flux densities vanish on the surface, which in connection with isotropic media means that the fields themselves do not have normal components: $\mathbf{n} \cdot \mathbf{E} = 0$ and $\mathbf{n} \cdot \mathbf{H} = 0$. Recent generalizations to the DB boundary condition include the so-called D'B' boundary [9, 10].

In the following, we will focus the analysis on the PEC boundary condition, and look for ways to simulate it by material structures.

III. ISOTROPIC EXTREME-PARAMETER MATERIALS

Let us limit the discussion to isotropic materials whose electromagnetic response can be characterized by two (complex) parameters, the relative permittivity ϵ_r and relative permeability μ_r.[1] Using these parameters, two other quantities can be written, the refractive index $m = \sqrt{\mu_r \epsilon_r}$ and the relative wave impedance $\eta_r = \sqrt{\mu_r / \epsilon_r}$. Then, depending on whether the magnitudes of any of these four parameters are very large (VL) or very small (NZ, "near-zero"), we can distinguish the eight classes of extreme-parameter electromagnetic media that are listed in Table 1.

Plotted in the plane where the axes give the logarithm of the permittivity and the permeability, the extreme-parameter materials are located away from the origin, as shown in Figure 2. The logarithm implies here that the parameters are assumed to have only positive values.

[1] The relative permittivity of the material is defined by normalizing the absolute permittivity ϵ by the free-space permittivity ϵ_0, likewise for the permeability: $\mu = \mu_r \mu_0$. The speed of light is $c = 1/\sqrt{\mu_0 \epsilon_0}$.

Table 1: Classes of extreme-parameter media

	very large	very small
ϵ_r	EVL	ENZ
μ_r	MVL	MNZ
m	IVL	INZ
η_r	ZVL	ZNZ

IV. ARTIFICIAL PEC MATERIAL

Intuitively, the concept of a perfect electric conductor is close to medium with a very large permittivity value. Indeed, a high permittivity means that the electric field inside the medium is forced to vanish in order not to run into an infinite energy density (which is proportional to $\epsilon_r|\mathbf{E}|^2$). Consequently, due to the continuity of the tangential electric field over the boundary, the tangential field has to vanish on both sides of the boundary. Hence, the PEC condition is satisfied on the surface of a material with $\epsilon_r = \infty$.

In addition, also from the point of electrostatics, a similar argument can be made. The image of a point charge from a dielectric half space of permittivity ϵ_r has the amplitude $-(\epsilon_r - 1)/(\epsilon_r + 1)$ compared to the original source [11, p. 111]. This image clearly approaches, when $\epsilon_r \to \infty$, the mirror image of a point charge from a PEC plane, which is of the same magnitude as the original charge but of opposite sign.

However, the situation is not as simple in electrodynamics. From Faraday's law in the electromagnetic time-harmonic case ($\nabla \times \mathbf{E} = -\mathrm{j}\omega\mathbf{B}$), one can infer that also the magnetic flux density $\mathbf{B}$ has to vanish inside a medium where the electric field is identically zero. Furthermore, the magnetic constitutive relation reads

$$\mathbf{B} = \mu\mathbf{H}. \tag{1}$$

While $\mathbf{B}$ is identically zero, no condition is set to the magnetic field strength. If finite values are allowed for the $\mathbf{H}$ field, the inevitable conclusion is that the permeability has to vanish: $\mu_r = 0$. Furthermore, due to the continuity of the normal-directed flux densities over interfaces, a corollary of the PEC condition would be that the normal component of the magnetic flux density is zero on this boundary: $\mathbf{n} \cdot \mathbf{B} = 0$.

This line of argument raises the question whether it is possible to replace a situation involving the mathematically idealized PEC condition by a homogeneous high-permittivity structure, or does one need to require an additional condition that the permeability is small. In the following, we examine the validity of the previous argumentation which calls for extreme values for both permittivity and permeability by solving electromagnetic scattering problems from such structures.

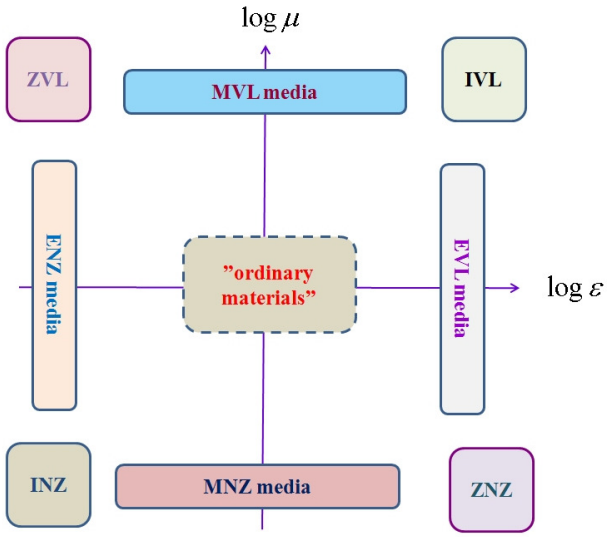

Fig. 2. Plotted in the plane where the axes are the logarithms of the (positive and isotropic) permittivity ϵ_r and permeability μ_r, the various classes of extreme materials fall away from the center. Depending on whether the permittivity (E), permeability (M), the refractive index (I), or the impedance (Z) is very small or very large, the different extreme-material parameters occupy a certain place in the plane.

V. SCATTERING BY EXTREME-PARAMETER OBJECTS

For small objects, the scattering by an electromagnetic plane wave can be explained by dipole scattering. For example, the Rayleigh scattering from a dielectric particle is due to an electric dipole whose amplitude can be calculated from the electrostatic excitation. It is, however, known in the Rayleigh-scattering regime [12, Section 8.25] that to replace a PEC object by an equivalent penetrable object, one needs to account for the magnetic dipole (calculated with $\mu_r = 0$), in addition to the electric dipole (with $1/\epsilon_r = 0$). For example, the scattering pattern of a purely dielectric (small) sphere has the same amplitude in both forward and backward directions, whereas a PEC sphere

has a dominating backscattering: the back-to-front ratio is close to 10 dB in the Rayleigh scattering regime [13].

In this section, we examine the scattering problem from extreme-parameter objects in more detail.

A. Mie scattering by a sphere

The scattering situation is of course more complicated when the scatterer is no longer small compared with the wavelength. For a homogeneous sphere, the problem can be solved using Mie theory [14, 15]. The scattered fields of a dielectric sphere with relative permittivity ϵ_r, relative permittivity μ_r, refractive index $m = \sqrt{\mu_r \epsilon_r}$, radius r, and size parameter $x = \omega r/c$, are expanded using the Mie coefficients a_n and b_n:

$$a_n = \frac{\epsilon_r \mathrm{j}_n(mx)[x\mathrm{j}_n(x)]' - \mathrm{j}_n(x)[mx\mathrm{j}_n(mx)]'}{\epsilon_r \mathrm{j}_n(mx)[x\mathrm{h}_n^{(2)}(x)]' - \mathrm{h}_n^{(2)}(x)[mx\mathrm{j}_n(mx)]'} \tag{2}$$

$$b_n = \frac{\mu_r \mathrm{j}_n(mx)[x\mathrm{j}_n(x)]' - \mathrm{j}_n(x)[mx\mathrm{j}_n(mx)]'}{\mu_r \mathrm{j}_n(mx)[x\mathrm{h}_n^{(2)}(x)]' - \mathrm{h}_n^{(2)}(x)[mx\mathrm{j}_n(mx)]'} \tag{3}$$

that involve spherical Bessel j_n and Hankel $\mathrm{h}_n^{(2)}$ functions and where the prime indicates differentiation with respect to the argument in parenthesis.

For a spherical domain, on the surface of which the PEC condition is forced, the corresponding coefficients can be derived:

$$a_n = \frac{[x\mathrm{j}_n(x)]'}{[x\mathrm{h}_n^{(2)}(x)]'} = \frac{x\mathrm{j}_{n-1}(x) - n\mathrm{j}_n(x)}{x\mathrm{h}_{n-1}^{(2)}(x) - n\mathrm{h}_n^{(2)}(x)} \tag{4}$$

$$b_n = \frac{\mathrm{j}_n(x)}{\mathrm{h}_n^{(2)}(x)}. \tag{5}$$

It is worth noting that Equations (4) and (5) also follow from the coefficients (2) and (3) in case $\epsilon_r \to \infty$, $\mu_r \to 0$, for a finite m.

Let us compare the Mie coefficients of the PEC sphere and same-sized spheres with extreme material parameters. Figure 3 shows the behavior of the first Mie scattering coefficient a_1 for a PEC sphere and two material realizations to approximate it. In the first of the cases, the relative permittivity is $\epsilon_r = 10^6$ and there is no magnetic response. The other one is less extreme in permittivity $\epsilon_r = 10^3$, but it has the relative permeability value of $\mu_r = 10^{-3}$.

The figure shows clearly that the most effective way to simulate the smooth PEC behavior by a penetrable sphere is using a medium with high-permittivity along with low-permeability, instead of a non-magnetic, solely extreme-permittivity response. In the case where the sphere is purely dielectric, there are numerous narrow resonances in the frequency dependence of the Mie coefficient which contaminate the curve (that in average follows the PEC function). In contrast, if the penetrable sphere becomes diamagnetic

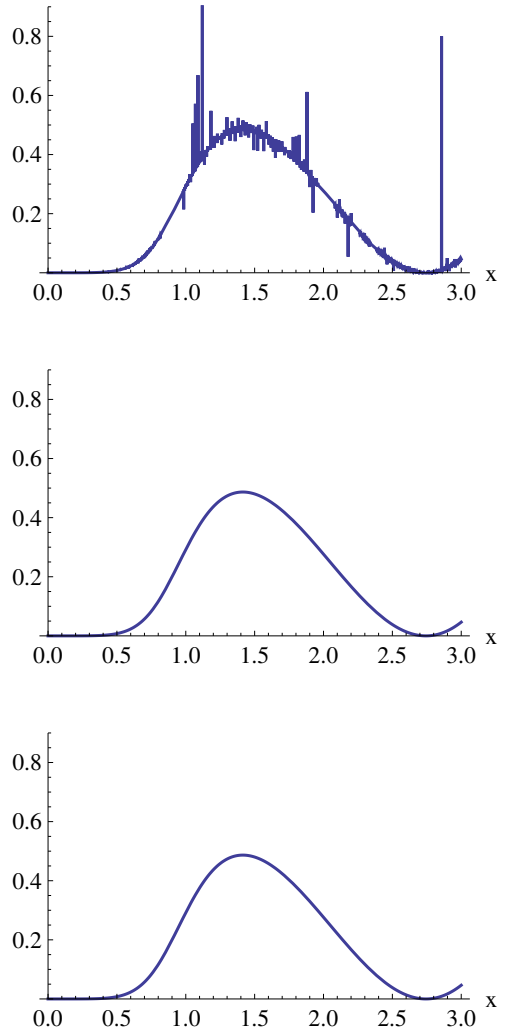

Fig. 3. Real part of the Mie coefficient a_1 as function of size parameter $0 < kr < 3$ for a non-magnetic dielectric sphere with $\epsilon_r = 10^6$ (top), a dielectric–magnetic sphere with $\epsilon_r = 10^3$ and $\mu_r = 10^{-3}$ (middle), and for a sphere on the surface of which the PEC condition is forced (bottom). The resolution of the picture is not able to display all the resonances in the topmost curve. However, it is anyway sufficient to show that the curve in the center figure is clearly a better approximation to the PEC than the topmost one.

($\mu_r < 1$), the PEC behavior is captured even if the permittivity and permeability parameters are not very extreme.

In other words, at least for this case of a sphere, the ZNZ model ($\eta_r = \sqrt{\mu_r/\epsilon_r}$ near zero) approximates PEC better than the EVL model (ϵ_r very large).

B. Scattering by a cube

A similar comparison can be made for the case when the scatterer is a cube. Figures 4 and 5 display the forward and backward scattering cross sections of various type of cubes: a PEC cube, and two penetrable cubes for which the permittivity increases. One of these cubes is purely dielectric, whereas the other's permeability decreases along with increasing permittivity. The size of the cube is comparable with the wavelength ($ka = 3$, with a being the side length), and the plane wave is incident head-on to one of the faces of the cube.

The scattering results have been calculated using the surface integral equation formulation where the scatterer is modeled either as a non-penetrable object with the PEC boundary condition or as a penetrable object. In the first case, the PEC condition, $\mathbf{n}\times\mathbf{E} = 0$, is enforced to the surface integral representation of the electric field and the solution is found with the electric field integral equation formulation [16, 17]. In this case, the fields inside the object are not modeled.

In the latter case, the scatterer is penetrable and the fields are modeled also inside the object. On the surface, the interface conditions, i.e., the continuity of the tangential electric and magnetic fields, are required and the solution is found with the Poggio–Miller–Chang–Harrington–Wu–Tsai (PMCHWT) formulation [18]. In both cases, the surface current densities are approximated with the triangular Rao–Wilton–Glisson (RWG) [16] basis functions, the equations are converted into matrix equations with Galerkin's testing procedure, and the matrix equations are solved with a direct method.

The message of the curves in the figures is clear. As the permittivity of the penetrable spheres increases, the scattering cross section approaches that of the PEC cube, both in the backward and forward scattering directions. However, the convergence for the purely dielectric cube is slow due to the jumps and resonances in the curve as the permittivity increases towards the EVL case. On the other hand, if the permeability decreases at the same time as the permittivity increases,

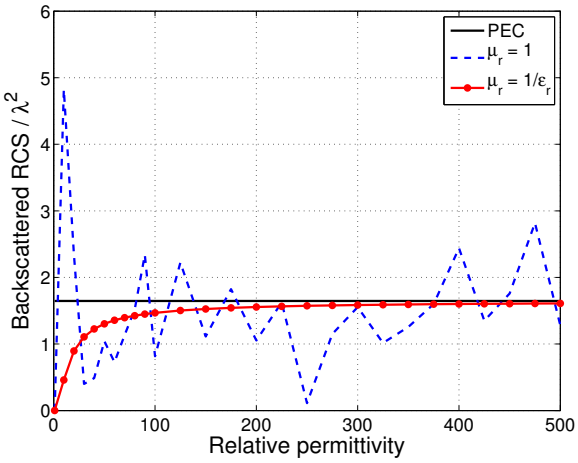

Fig. 4. The normalized backscattering cross section of a PEC cube ($ka = 3$), compared with penetrable cubes of the same size but of varying permittivity. One of the cubes is purely dielectric and the other has also diamagnetic response. The cross section is normalized by wavelength squared.

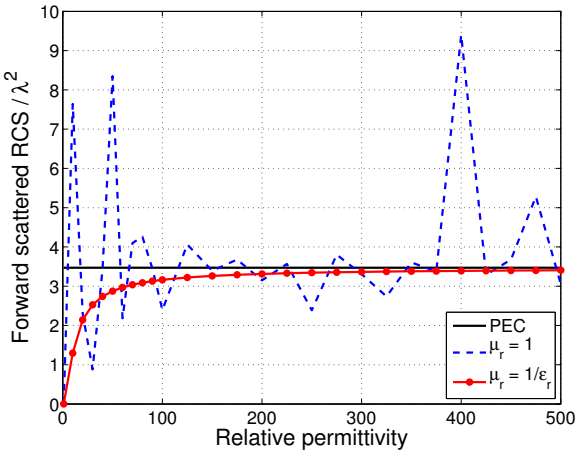

Fig. 5. The same as in Figure 4, the forward scattering cross section.

the scattering coefficients approach very soon those of the PEC cube. For instance, when $\epsilon_r = 1/\mu_r = 500$, the relative difference in the cross section is a couple of percents.

The EVL case ($\epsilon_r \to \infty$, $\mu_r = 1$) is numerically challenging, because the wave number inside the object becomes very large and the Green's function highly oscillating. This may partially explain the jumps in the curves in Figures 4 and 5. In the other case, (ZNZ, $\epsilon_r \to \infty$ and $\mu_r = 1/\epsilon_r$), the refractive index $m = \sqrt{\epsilon_r\mu_r}$ is unity and the problem is much easier to solve with numerical methods.

C. Effect of losses

In microwave and radio engineering, a common practice is to assume that good conductors, for example copper or some other metals, behave reasonably as approximations for PEC. In the frequency domain, the effect of conductivity σ comes through the imaginary part of the permittivity ($\mathrm{Im}\,\epsilon = -\sigma/\omega$). This raises the question whether the ideal PEC behavior can be synthetized more effectively when the imaginary part—instead of the real part—of the permittivity becomes very large.

In Figure 6, we compare the scattering efficiencies of various spheres (with size parameter $kr = 1$) against the ideal PEC sphere. The scattering efficiency is a dimensionless parameter, defined as the integrated total scattering cross section divided by the geometrical cross section of the scatterer. We plot the absolute difference of the efficiency of the PEC sphere and that of the material sphere when the material parameters grow to very large values. Three different cases are treated: purely dielectric ($\epsilon_r \to \infty$), dielectric–magnetic ($\epsilon_r \to \infty, \mu_r \to 0$), and electrically dissipative ($\sigma \to \infty$).

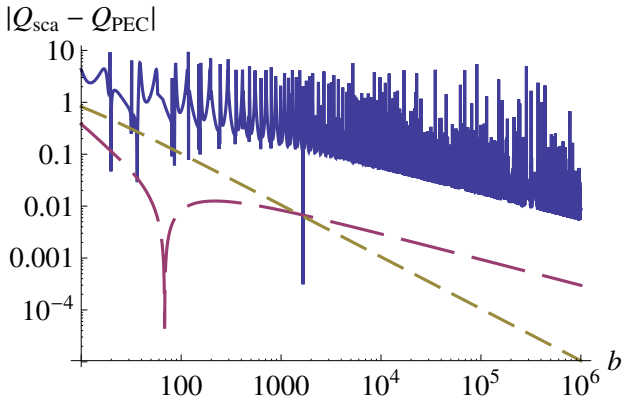

Fig. 6. The absolute value of the difference between the scattering efficiency of a PEC sphere and three material realizations: dielectric sphere ($\epsilon_r = b, \mu_r = 1$, solid line), dielectric–magnetic sphere ($\epsilon_r = 1/\mu_r = b$, short-dashed line), and dielectrically lossy sphere ($\epsilon_r = 1 - \mathrm{j}\,b, \mu_r = 1$, long-dashed line). The size of the sphere is $kr = 1$.

The curves show that when the parameter b grows to very large values, all material realizations approach the PEC case in terms of the scattering efficiency. As was seen also earlier (Figure 3), the purely dielectric sphere exhibits narrow resonances which destroy its possibilities of being a very good PEC approximation. Furthermore, even if the resonances were filtered away from this curve, the error would still decrease rather slowly. The ZNZ curve (large permittivity along with small permeability) approaches much faster the PEC state than the baseline of the EVL curve.

In the case of the conducting sphere in which the imaginary part of the permittivity grows, no resonances are seen, which is also expected. Also, the error in approximating PEC scattering becomes smaller for increasing conductivity. However, the speed at which the error becomes smaller is clearly lower that of the EVL curve. Numerically it can be shown that the asymptotic behavior of the latter (ZNZ) one is b^{-1} whereas the curve showing the error of the conducting sphere decreases as $b^{-1/2}$.

A further disadvantage of the model of the PEC object as an extreme conductor is that for a conducting scatterer, the extinction is larger than the scattering cross section. This is due to the dissipation of the fields that penetrate within the skin depth of the object which means that absorption adds up to scattering with the result that extinction increases. Hence the comparisons of the scattering cross section and the extinction cross section against the PEC case yield different results. In this respect, the ZNZ object is much closer to the PEC object; both ZNZ and PEC lack absorption and therefore have unit albedo.

Figure 7 displays the albedo (defined as the ratio of the scattering cross section to the extinction cross section [19, p. 183]) of a dielectric, lossy sphere (size parameter $kr = 1$) as a function of the imaginary part of the permittivity. The figure shows that the scattering and extinction can be clearly different, even if it is true that for low losses on one hand and high losses on the other, the albedo approaches unity.

D. Single and double negative permittivity

For metals at microwave frequencies, the approximation of a very large imaginary part of the permittivity is well-founded. However, far higher in the frequency range, the imaginary part of metal permittivity decreases according to the Drude dispersion model, and the dominating character of the dispersion is the negative real part of the permittivity [20]. This fact suggests one further possibility to mimic PEC objects: with negative-permittivity scatterers.

Figure 8 displays the scattering efficiencies of various spheres with size parameter $kr = 3$ as a function

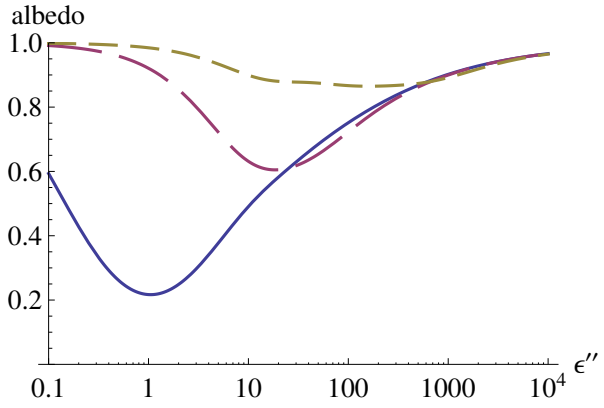

Fig. 7. The albedo (scattering efficiency divided by extinction efficiency) of a lossy dielectric sphere as a function of the (negative) imaginary part of the permittivity. Solid line: $\epsilon = 2 - \mathrm{j}\epsilon''$, long-dashed line: $\epsilon = 50 - \mathrm{j}\epsilon''$, short-dashed line: $\epsilon = 1000 - \mathrm{j}\epsilon''$. The sphere size is $kr = 1$.

of increasing medium parameter values. In addition to the dielectric–magnetic and lossy objects, also single and double-negative permittivity scatterers are shown.

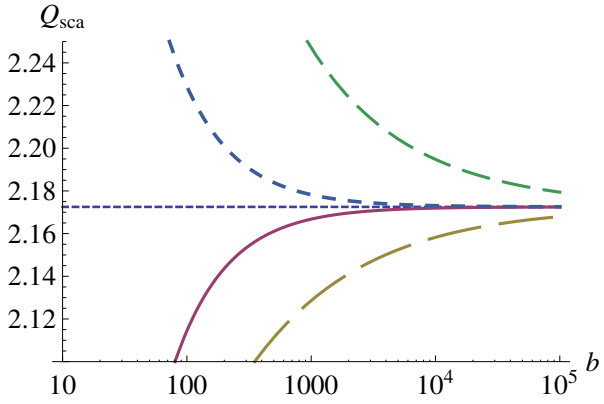

Fig. 8. The scattering efficiencies of four spheres: dielectric–magnetic sphere ($\epsilon_r = b, \mu_r = 1/b$, solid line), dielectrically lossy sphere ($\epsilon_r = 1 - \mathrm{j}\,b, \mu_r = 1$, long-dashed), single-negative sphere ($\epsilon_r = -b, \mu_r = 1$, medium-dashed), and double-negative sphere ($\epsilon_r = -b, \mu_r = -1/b$, short-dashed). The size of the sphere is $kr = 3$. The dotted line shows the PEC value.

We can observe from the curves that a negative-permittivity scatterer does not perform better in approximating the PEC response than the lossy scatterer (with large imaginary permittivity). However, if also the permeability is negative and small, in addition to the large and negative permittivity, the scattering efficiency approaches more effectively that of the PEC sphere, and the convergence speed is the same as for the positive dielectric–magnetic (ZNZ) sphere.

VI. DISCUSSION

The previous analysis has focused on the difference between the boundary problem and the interface problem. One needs to make a clear distinction between ideal boundaries on one hand and material interfaces on the other. Boundary conditions can serve as approximations to inhomogeneous real world structures (analytic approach) and vice versa: one can try to mimic boundary conditions using electromagnetic materials (synthetic approach). To be able to approximate boundary conditions, extreme-parameter materials were needed.

The clear message of the analysis is that to simulate a PEC object by a homogeneous isotropic material object, it is most efficient to use a material with simultaneously large permittivity *and* small permeability, instead of a pure dielectric medium with either high permittivity or high conductivity. In other words, a ZNZ ("near-zero impedance") medium is better than an EVL ("epsilon-very-large") medium.

It is important to note that in addition to the requirement of small value for the relative impedance in the ZNZ picture, there is an additional degree of freedom in the extreme-medium desciption: the refractive index m. In the calculations of this study, m was taken as unity. This is not compulsory. In fact, the errors in scattering magnitudes of ZNZ objects compared against PEC are functions of m. However, it seems that the best value of m of a ZNZ scattering in simulating PEC behavior is always quite close to unity, even if not exactly. The optimum depends on the shape and size of the object.

This result about the PEC–ZNZ connection can be generalized to perfectly magnetic conductors. Even if the analysis did not treat PMC boundary conditions, we can make use of the duality between electric and magnetic quantities in Maxwell equations and conclude that a material realization for a PMC boundary is a "very large impedance" (ZVL) material rather than a "mu-very-large" (MVL) medium.

One important question in trying to simulate boundary conditions with electromagnetic materials is uniqueness. The synthesis of a given boundary condition does not necessarily lead to unique recipes. The fabrication of a DB boundary (the normal components

of the electric and magnetic flux densities are forced zero) is an example showing the degrees of freedom in this respect. To create the effect of a DB surface, one possibility is to take uniaxial material in which the permittivity and permeability eigenvalues vanish in the axial direction. If such a material is cut so that the interface is perpendicular to the optical axis, the normal components of both the electric and magnetic flux densities are forced to vanish on the surface.

However, as shown in [21], another choice to create a DB boundary is by use of the so-called IB material. The IB medium, also termed as skewon–axion medium [22], is characterized by a four-dimensional material tensor dominated by the antisymmetric part with the additional PEMC parameter. The number of medium parameters in the general IB medium is 16, meaning that there are several degrees of freedom in the construction of a materials to give rise to a DB boundary.

The uniqueness question can, also, be raised in connection of the PEC synthesis. The condition on the PEC boundary is that the *tangential* electric field vanish. On the other hand, due to the continuity of the tangential electric field across an interface, it suffices to force the tangential electric field within the synthetized medium to vanish. Allowing for an anisotropic medium, this can be done by letting the tangential component of the permittivity dyadic grow to infinity (and, at the same time, the normal component of the permeability dyadic decreases to zero). Such an anisotropic medium would be another choice, in addition to the isotropic ZNZ medium, to simulate the PEC behavior.

Another aspect of the question of uniqueness of the PEC realization concerns the realization of infinite material parameters. The numerical calculations in this article have indicated that there are several different material realizations (for example, EVL, ZNZ, well-conducting, double-negative, etc.) of media which all in the extreme limit approach the PEC behavior. In this sense, the PEC realization can be considered non-unique. However, the message is that for pragmatic and numerical purposes, the ZNZ method to mimic PEC behavior is computationally most effective.

ACKNOWLEDGMENT

This study has been supported by the Academy of Finland, through grants 108801 and 124204.

REFERENCES

[1] A. Sihvola, S. Tretyakov, and A. de Baas, "Metamaterials with extreme material parameters," *Journal of Communications Technology and Electronics*, vol. 52, no. 9, pp. 986–990, 2007. Also published (in Russian): Metamaterialy s ekstremal'nymi material'nymi parametrami, *Radiotekhnika i elektronika*, vol. 52, no. 9, pp. 1066–1071, 2007.

[2] M. G. Silveirinha, A. Alù, B. Edwards, and N. Engheta, "Overview of theory and applications of Epsilon-Near-Zero materials," in *Proceedings of URSI XXIX General Assembly*, International Union of Radio Science, Chicago, USA, August 2008. Paper *B01p6*.

[3] G. Pelosi and P. Ufimtsev, "The impedance-boundary condition," *Antennas and Propagation Magazine, IEEE*, vol. 38, pp. 31–35, Feb 1996.

[4] I. V. Lindell and A. H. Sihvola, "Perfect electromagnetic conductor," *Journal of Electromagnetic Waves and Applications*, vol. 19, no. 7, pp. 861–869, 2005.

[5] A. Sihvola and I. V. Lindell, "Perfect electromagnetic conductor medium," *Annalen der Physik (Berlin)*, vol. 17, no. 9-10, pp. 787–802, 2008.

[6] P.-S. Kildal, "Definition of artificially soft and hard surfaces for electromagnetic waves," *Electronics Letters*, vol. 24, pp. 168–170, Feb 1988.

[7] V. Rumsey, "Some new forms of Huygens' principle," *Antennas and Propagation, IRE Transactions on*, vol. 7, pp. 103–116, December 1959.

[8] I. V. Lindell and A. H. Sihvola, "Electromagnetic boundary and its realization with anisotropic metamaterial," *Physical Review E (Statistical, Nonlinear, and Soft Matter Physics)*, vol. 79, no. 2, p. 026604, 2009.

[9] I. V. Lindell and A. H. Sihvola, "Electromagnetic boundary conditions defined in terms of normal field components," *Antennas and Propagation, IEEE Transactions on*, vol. 58, pp. 1128–1135, april 2010.

[10] I. V. Lindell, H. Wallén, and A. Sihvola, "General electromagnetic boundary conditions involving normal field components," *Antennas and Wireless Propagation Letters, IEEE*, vol. 8, pp. 877 –880, 2009.

[11] J. G. V. Bladel, *Electromagnetic Fields*. Hoboken, New Jersey: Wiley-Interscience, sec-

ond ed., 2007.

[12] D. S. Jones, *The theory of electromagnetism*. Oxford: Pergamon Press, 1964.

[13] A. Sihvola, P. Ylä-Oijala, and I. V. Lindell, "Scattering from a PEMC (perfect electromagnetic conductor) spheres using surface integral equation approach," *Applied Computational Electromagnetics Society Journal*, vol. 22, pp. 236–249, July 2007.

[14] G. Mie, "Beiträge zur Optik trüber Medien, speziell kolloidaler Metallösungen," *Annalen der Physik*, vol. 25, pp. 377–445, 1908.

[15] C. F. Bohren and D. R. Huffman, *Absorption and Scattering of Light by Small Particles*. New York: Wiley, 1983.

[16] S. Rao, D. Wilton, and A. Glisson, "Electromagnetic scattering by surfaces of arbitrary shape," *Antennas and Propagation, IEEE Transactions on*, vol. 30, pp. 409–418, May 1982.

[17] V. Jandhyala and S. Chakraborty, "Surface-based integral equation formulations for multiple material and conducting objects," *Applied Computational Electromagnetics Society Newsletter*, vol. 20, pp. 25–47, November 2005.

[18] K. Umashankar, A. Taflove, and S. Rao, "Electromagnetic scattering by arbitrary shaped three-dimensional homogeneous lossy dielectric objects," *Antennas and Propagation, IEEE Transactions on*, vol. 34, pp. 758–766, June 1986.

[19] H. C. van de Hulst, *Light scattering by small particles*. New York: Dover, 1981.

[20] S. A. Maier, *Plasmonics: Fundamentals and applications*. New York: Springer, 2007.

[21] I. V. Lindell and A. H. Sihvola, "Uniaxial IB-medium interface and novel boundary conditions," *Antennas and Propagation, IEEE Transactions on*, vol. 57, pp. 694–700, March 2009.

[22] F. W. Hehl and Y. N. Obukhov, *Foundations of Classical Electrodynamics*. Boston: Birkhäuser, 2003.

Ari Sihvola was born on October 6th, 1957, in Valkeala, Finland. He received the degrees of Diploma Engineer in 1981, Licentiate of Technology in 1984, and Doctor of Technology in 1987, all in Electrical Engineering, from the Helsinki University of Technology (TKK), Finland. Besides working for TKK and the Academy of Finland, he was visiting engineer in the Research Laboratory of Electronics of the Massachusetts Institute of Technology, Cambridge, in 1985–1986, and in 1990–1991, he worked as a visiting scientist at the Pennsylvania State University, State College. In 1996, he was visiting scientist at the Lund University, Sweden, and for the academic year 2000–01 he was visiting professor at the Electromagnetics and Acoustics Laboratory of the Swiss Federal Institute of Technology, Lausanne. In the Summer of 2008, he was visiting professor at the University of Paris XI, France. Ari Sihvola is professor of electromagnetics in Aalto University School of Science and Technology (before 2010, Helsinki University of Technology) with interest in electromagnetic theory, complex media, materials modelling, remote sensing, and radar applications. He is Chairman of the Finnish National Committee of URSI (International Union of Radio Science) and Fellow of IEEE. He also served as the Secretary of the 22nd European Microwave Conference, held in August 1992, in Espoo, Finland. He was awarded the five-year Finnish Academy Professor position starting August 2005.

Ismo Lindell was born in 1939 in Viipuri, Finland. He received his degrees of Electrical Engineer (1963), Licentiate of Technology (1967), and Doctor of Technology (1971), at the Helsinki University of Technology (HUT), Espoo, Finland. In 1962, Dr. Lindell joined the Electrical Engineering Department of HUT, since 1975 as Associate Professor of Radio Engineering and, since 1989, as Professor of Electromagnetic Theory at the Electromagnetics Laboratory which he founded in 1984. During a sabbattical leave in 1996-2001, he held the position of Professor of the Academy of Finland. Currently, he is Professor Emeritus at the Department of Radio Science and Engineering within the Faculty of Electronics, Telecommunications and Automation of the School of Science and Technology in Aalto University. Dr. Lindell enjoyed the Fulbright scholarship as a visiting scientist at the University of Illinois, Champaign-Urbana in 1972-1973 and the Senior Scientist scholarship of Academy of Finland at the M.I.T., Cambridge, in 1986-1987. Dr Lindell has authored and coauthored 265 scientific papers and 12 books, for example, *Methods for Electromagnetic Field Analysis* (IEEE Press, New York 3rd printing 2002), *Electromagnetic Waves in Chiral and Bi-Isotropic Media* (Artech House, Norwood MA, 1994), *Differential Forms in Electromagnetics* (Wiley and IEEE Press, New York 2004), and *Long History of Electricity* (Gaudeamus, Helsinki, Finland 2009, in Finnish). Dr. Lindell has received the IEEE S.A. Schelkunoff award (1987), the IEE Maxwell Premium (1997 and 1998) and the URSI van der Pol gold medal in 2005 as well as the State Award for Public Information (2010).

Henrik Wallén was born in 1975 in Helsinki, Finland. He received the M.Sc. (Tech.) and D.Sc. (Tech.) degrees in Electrical Engineering in 2000 and 2006 from the Helsinki University of Technology (which is now part of the Aalto University).

He is currently working as a Postdoctoral Researcher at the Aalto University School of Science and Technology, Department of Radio Science and Engineering in Espoo, Finland. He is Secretary of the Finnish National Committee of URSI (International Union of Radio Science). His research interests include electromagnetic theory, modeling of complex materials, and computational electromagnetics.

Pasi Ylä-Oijala received the M.Sc. and Ph.D. degrees in applied mathematics from the University of Helsinki, Helsinki, Finland, in 1992 and 1999, respectively. Currently, he is a Finnish Academy Research Fellow with the Aalto University, School of Science and Technology, Department of Radio Science and Engineering, Finland. His field of interest includes integral equation and fast methods in computational electromagnetics.